Advanced and Sustainable Technologies
ASET
E-ISSN 2976-2294
Volume 5, No 1, June 2026 [262-273]

Reconstruction of Broken Parts Utilizing 3D Printing

Muntaka Musa[1] and Ahmad Baharuddin Abdullah[1]*

[1]Metal Forming Research Laboratory, School of Mechanical Engineering, Universiti Sains Malaysia, 14300 Nibong Tebal, Pulau Pinang, Malaysia.

Received 13 December 2026, Revised 7 February 2026, Accepted 25 February 2026

ABSTRACT

One of the applications of 3D printing, like fused deposition modelling (FDM), is for the reconstruction of broken parts or features. The reconstruction of a part or feature proceeds mainly to extend its life cycle. The most common challenges in the reconstruction include achieving acceptable dimensional accuracy and good surface roughness. In this project, the focus is to observe the effect of process parameters, like layer heights to the dimensional accuracy and surface finish. Four layer heights (0.1, 0.2, 0.3, and 0.4 mm) are used, and other parameters such as wall thickness, printing temperature, hot-bed temperature, print speed, and infill density are set to 0.8 mm, 2200C, 50.0 0C, 80.0 mm/s, and 20%, respectively. This study begins by generating a digital model of the broken features, followed by modification of the G-code program, and ends with a repair operation by printing the broken features on the real part. A plastic gear was used as a case study. These results showed high dimensional accuracy, with deviations of 10 to 1 microns at a layer height of 0.2 mm. Similarly, acceptable surface roughness was observed at a layer height of 0.2 mm, with an average and root-mean-square roughness of Ra-21.2392µm and Rq-25.6308µm, respectively. The developed method shows a very promising approach to be applied in various applications.

Keywords: Extend part life cycle, Digital model, Reconstruction, Dimensional accuracy.

1. INTRODUCTION

The constructed waste 3D parts or features, especially those made from plastic, should be recycled if they are damaged or broken and found in the garbage. The materials can be digitally revitalized for repairs, reduce dependency and extend their lifespan. Many techniques are being employed with this technology in industries such as aerospace and automobiles. Facilities, applications/software, manufacturing, designs, and materials are some of the processes used to repair complex parts. Polymers are becoming widespread as engineering materials because of their importance like easy to recycle, strong, cost-effective, and used for repairing damaged 3D parts [1]. If the methods are enhanced, the repaired models will revert to normality and function efficiently. The prevalent parts are difficult to find and need to be repaired [2]. They may be hard to employ 3D scanning to precisely fabricate complex 3D parts [3]. It was found that without contact of parts, 3D scanning can be applied to acquire objects digitally [4, 5, 6]. The 3D models can be produced rapidly when detailed point cloud data is captured during the scanning process [7]. This demonstrates an innovative approach to problem identification and analysis, resulting in a complete gear part model that makes the reconstruction process more effective.

The advancement of 3D printing techniques using plastic and metal materials provided a basis for research that facilitates the construction of high-value components [8]. This was discovered that AM utilizes a 3D Computer-aided design model to produce complex parts by a layer-by-layer process [9, 10, 11, 12]. The methods include fused filament fabrication (FFF)/fused deposition

*Corresponding author: mebaha@usm.my

modelling (FDM) [13, 1], stereolithography (SLA) [14], laser directed energy deposition DED) [15], digital light processing (DLP) [16], etc. The emphasis was on using a 3D printing machine, with different materials automatically used in the manufacturing process to achieve repairs [1]. The study found that repair is a method of reproducing the defective part to restore its normal function and extend its lifespan 15]. So, it is essential to empty the trash that contains damaged and broken parts. This will boost waste management, alleviate environmental emission issues, and recycle such components for industry restoration, like in aerospace, automobile, and health sectors. Having studied many approaches, it was observed that FDM technology is among the most widely used because it is cost-effective, makes printing with PLA easier, and has a moderate system. In this study, a plastic gear was used to reconstruct the broken feature using FDM technology. The outlines for reconstructing the missing gear tooth, such as preparation of materials, 3D scanning, modelling and 3D printing, process parameters - layer heights (0.1mm to 0.4mm), measurement of dimensional accuracy DA and surface roughness (SR) would be highlighted. Post-processing, comparison of reconstructed features with the original ones, and cost-benefit analysis would also be discussed.

The study finds a possible way to improve damaged/broken reconstruction and restore the normalcy of the gear model. This is due to the role of plastic gear in human endeavours, which is developing rapidly, making the repair of defective parts indispensable.

2. MATERIAL AND METHODS

The objective of the study is to employ the methods of reconstruction of broken features using 3D printing, as outlined in Figure 1:

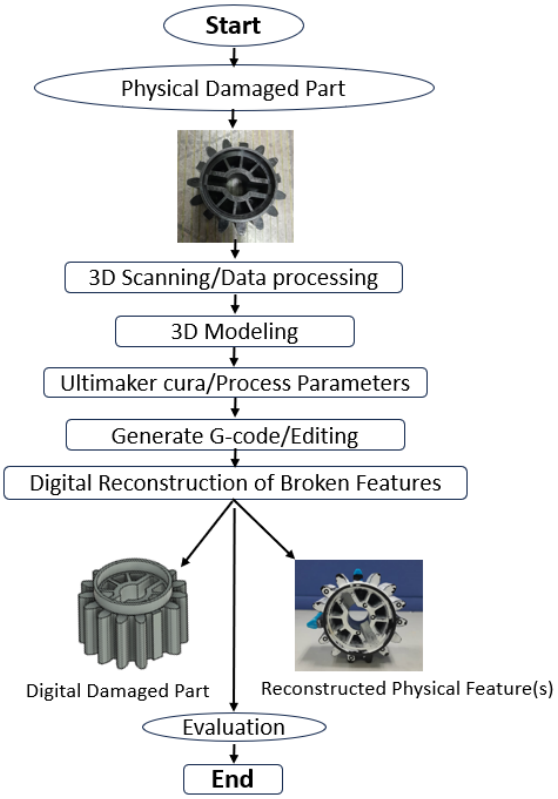

Figure 1: General flow chart for reconstruction of broken features.

2.1 Determine the Damaged Features

The availability of materials is the primary justification for carrying out this research on the complex geometry of the model, its functions [2], etc. These were carefully observed, and it was decided to use a damaged gear model as a case study and as one of the high-value components. It was identified that traditional gear reconstruction is outdated, prompting the need to improve the digital approach due to the significance of plastic gears. One of the most important methods for constructing part models to digitally manufacture the complete shape of a physical object [17]. To determine the damaged part's dimension accuracy and reconstruct the missing gear tooth are the main issues. This technology is expected to be an effective method for reconstructing broken features onto the affected areas of the physical model.

2.2 Preparation of Physical Model

A bristle brush was used to clean dust, grease, and roughness from the physical gear model, which could affect data capture during scanning. The software utilized includes:

a) 3D Scanner (Ultra HD)

The ULTRA HD NextEngine 3D Scanner allows it to precisely measure distances on an object's surface with laser light, producing a digital 3D model. Its specifications are highlighted by [18].

b) Autodesk Fusion 360 Software

Autodesk Fusion 360 is a software program used for industrial and mechanical design. It allows the design of 3D models and the modification and validation of mechanical surfaces for design and engineering purposes.

2.3 3D Scanning and Model Digitization

One key step that closes the gap is data processing between capturing a physical object with a 3D scanner and obtaining a digital model. In the process, the digital gear representation will be produced by capturing data on the physical structures and their surroundings[19]. The collection of data increases the standard for innovative methods and digital part model repairs [20]. The study shows entire processes that improved the high precision for reconstructing the plastic gear model. The scanner's and desktop's connectivity make scanning easier and capture the entire data of the model effectively. The turntable holding the physical model and the 3D-scanned model's structure in the desktop settings is shown in Figure 2.

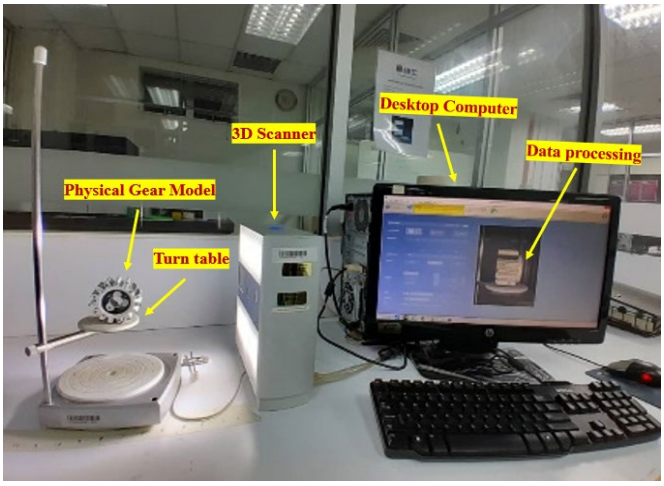

Figure 2: Desktop computer showing the connectivity and data processing.

Technical processes for feature reconstruction using a 3D scanner are: (a) Positioning, (b) Divisions, (c) Scanning Resolutions (Points/IN), (d) Target (colour), (e) Range and (f) Time. The physical 3D model was firmly positioned on the scanner's turntable for digital reconstruction using a 3D Scanner, with high resolution and recording millions of points [21]. It provides 3 types of scanning modes – (i) 360°, (ii) bracket, and (iii) single. The intricate geometry of 3D parts led to the careful selection of the 360° mode to ensure complete surface treatment. The scanner's turntable in Figure 3a rotated the model, and all sides were automatically captured. Some of the captured models presented in Figures 3b, 3c, and 3d showed some sides of the digital reconstructions of the 3D scans from the physical model.

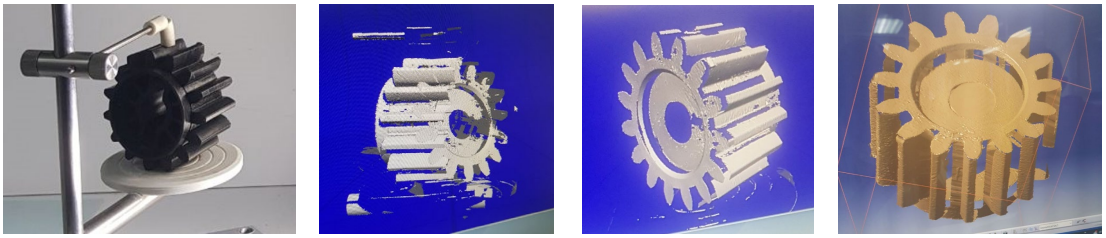

(a) (b) (c) (d)

Figure 3: (a) Physical gear model on Scanner's turntable (b) Digital model is oriented towards the right. (c) Digital model is oriented towards the left and (d) The digital model's orientation is upward.

The Standard Definition (SD) was used for scanning, approximately 4,400 points per inch was created to balance detail and processed data. To properly detect surfaces in dark mode, the natural color calibration was used to achieve the finest light reflection. The macro scan range was chosen to achieve higher accuracy and prevent misrepresentation from wider scans. Multiple scans and rotation increments were performed using a mechanical turntable from 7" to 25" inches. This simplified view of the digital model was obtained from multiple locations and required 13.6 to 15 minutes of scanning. The 3D model was successfully reconstructed digitally and saved as an STL file. file format.

2.4 3D Modelling, refinement and Quality Control

3D modeling is the technique of using software to create a representation of a 3D object; the major operations applied in modelling include rotation, scaling, bending, and removal of surface errors. Autodesk Fusion 360 is used in the CNC lab. played an important role in converting scan data to a digital model. The model's geometry was adjusted by trimming edges and repairing gaps to make the mesh object uniform [22]. Scan data refinement is one of the steps prior to 3D printing. The good refinement of a 3D model is essential in 3D scanning technology [23]. The surfaces of the digital gear model were checked, refined as in Figure 4a to validate its accuracy, integrity, and ensure its quality, and compared to the original plastic gear to ensure that key features and dimensions were maintained. Figure 4b shows the gear dimension; Figure 4c shows a broken feature; and Figures 4d and 4e are isometric/sectional views withome labeling in Table 2 [24].

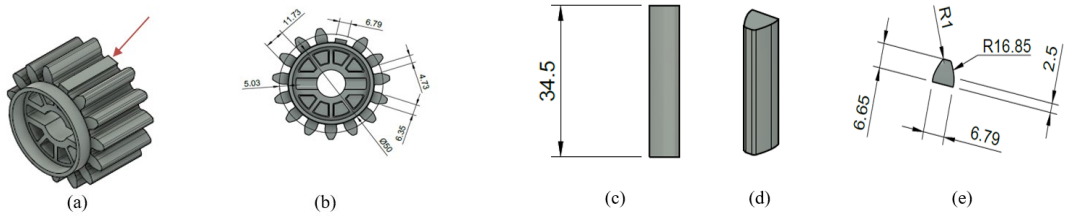

(a) (b) (c) (d) (e)

Figure 4: (a) Refined reconstructed digital model, (b) Gear dimensions, (c) Broken tooth's front view, (d) Isometric view and (e) Sectional views. (All unit is in mm)

Table 2: Descriptions of Markings.

S/no.	a. **Gear Dimension**	S/no.	b. **Broken Tooth - Top View**	S/no.	c. **Broken Tooth**
i.	11.73mm - Circular pitch	i.	6.65mm - Height	i.	34.5mm - Front view
ii.	5.03mm - Feet height	ii.	1mm - Radius (R_1)		
iii.	Ø 5.0mm - Diameter	iii.	16.85mm-Radius (R_2)		
iv.	6.35mm - Tooth thickness	iv.	2.5mm -Broken area (base)		
v.	4.73mm - Space width				
vi	6.79mm - Broken Area				

Based on this development, it was determined that the model to be reconstructed using a Creality Ender Plus 3D printer and Ultimaker Cura slicing software.

2.5 Exporting the Digital Model

The process continues by exporting the digital model as a Standard Tessellation Language (STL) or Stereolithography (STL) file to complete 3D printing. Hence, 3D modeling was successfully made and validated for other processes.

2.6 SolidWorks and Ultimaker Cura software

The design was created using CAD software, the models were compared to determine the parameters, and the results were obtained [25]. At the lab, for 3D printing, SolidWorks, a tool for constructing part models, was also used to cross-check and validate the reliability of the digital model [26, 27]. The file was transferred to Ultimaker Cura (slicing software) that supports STL. [28, 29, 30].

3. PROCESS PARAMETERS

The significant process parameters are layer heights to the dimensional accuracy and surface finishing with four levels (0.1, 0.2, 0.3 and 0.4 mm). They are considered as variables which are expected to show the outcomes, and other parameters [31] such as (see table 3) - wall thickness, printing temperature, hot-bed temperature, print speed, and infill density are constant at 0.8 mm, 2200C, 50.0 0C, 80.0 mm/s and 20% respectively. The adjustments and modifications to pause at height, other parameters, and the positions of digital parts in the Cura workflow were made, and the model was sliced and converted into G-code automatically so it could be printed in layers [32]. However, the damaged part was imported into the same Cura workflow, which shows it first orientation, after which it was rotated and moved to the selected position of the damaged part model. The x, y, and z axes had values of 134.0765 mm, 90.3244 mm, and 0 mm before the (drop-down model) model was positioned.

Table 3: Printing Process Parameters and their Values.

No.	Layer Height	0.1 mm	b	Layer Height	0.3 mm	c	Layer Height	0.4 mm
1	Wall thickness	0.8 mm	1	Wall thickness	0.8 mm	1	Wall thickness	0.8 mm
2	Printing Temp.	220.0 0C	2	Printing Temp.	220.0 0C	2	Printing Temp.	220.0 0C
3	Hot-Bed Temp.	50.0 0C	3	Hot-Bed Temp.	50.0 0C	3	Hot-Bed Temp.	50.0 0C
4	Print Speed	80.0 mm/s	4	Print Speed	80.0 mm/s	4	Print Speed	80.0 mm/s
5	Infill Density	20%	6	Infill Density	20%	6	Infill Density	20%

The first orientation of the broken feature, prior to proper positioning onto the damaged surface area of the part, was shown, with the broken feature toward the final position of the part displayed during the process. Then, after it was unchecked, the values for the broken feature part on the damaged surface were 129.5723 mm, 90.0536 mm, and 61.2236 mm (x, y, and z). However, the part's full assembly, preview, and broken feature were shown after the removal of the damaged part, with a layer height of 0.1mm indicating a total number of 35 layers, 0g and six (6) minutes duration of printing. Additionally, 5 minutes - 1g for 0.2mm represented 17 layers, and 0.3mm - 1g and 0.4mm - 1g each represented 11 and 9 layers, indicated with 3 minutes each.

3.1 G-code Programing/editing

The G-code file is a raw material used for a fused filament fabrication (FFF) printer to construct 3D parts [33]. It is used for sending an instruction to the machine (3D printer) [34]. Hence, it is a programming, it aids significantly in the printing process. In this study, the G-code of the damaged part (gear model) was not edited; it served as a base for positioning of the broken feature (gear teeth). While the g-code for the full assembly part was generated primarily to compare with that of the broken feature. This was formed by using "Notepad." Following the comparison, the pause at height was changed to 70 mm, which allows the nozzle to trace and begin layering from the damaged surface area of the part. However, the g-code of the broken feature was opened and traced the "Move to start position "area. The Y values, i.e., 20, 200, 200, and 20, were automatically displayed and adjusted to Y values of 120, 250, 250, and 120, respectively. The changes were made to prevent the damaged part from colliding with the 3D printer's nozzle.

Later, the initial layer of the broken feature in the g-code was displayed and labelled with Layer counts of each g-code i.e. 35, 17, 11, and 9 representing layers (0.1 mm, 0.2 mm, 0.3 mm, & 0.4 mm), and default Z-positions (layer:0). After that, all Z-position values were changed from Z0.2 to Z70.2 which matched the heights of the damaged parts in their complete assemblies. This ensured the 3D printer correctly read the g-code and began reconstructing the broken feature at Z-level 70.2, adding 0.2 layers up to the last number. After that, the G-code was saved as a file with a broken feature so that 3D printing might proceed.

4. RESULTS AND DISCUSSION

4.1 Reconstruction of Broken Feature Parts

Fused deposition modelling technology was used to produce high-quality printed products, and the results showed that the majority of the shapes had good accuracy, with a variation of less than 5% [35]. The samples were manufactured using the FDM 3D process and PLA material at various parameters, including layer heights [36]. The data revealed that layer height and extruder temperature are the most significant factors in DA. Therefore, in this study, the FDM method and PLA material were employed to digitally reconstruct small broken features onto the physically damaged parts of the model. The milling machine at the CNC lab was used to cut four (4) features (sizes: 3.46mm) from the original part (gear model) for repairs. However, the additional materials used are for the construction of a fixture to support the part and are manufactured with FDM technology [37]. Sandpaper was used to sand the damaged area for proper adhesion [38], and the other medium applied was epoxy (adhesive glue) to fix the printed feature [39].

Figures 6a and 6b display a custom-made fixture for mounting the gear during printing. The 3D printer (Creality Ender 5 Plus) was operated to manufacture parts or features [40], focusing to achieving high dimensional accuracy. The process began with importing saved files (damaged parts and broken features) into the 3D printer. After preheating the nozzle to 220.0°C and setting the hot bed to 50.0°C, the printer was turned on before beginning construction. It was turned on for x, y, and z printer travel to produce preliminary testing layers. While in, demonstrated an

attempt to fix the broken feature and to reconstruct the broken features (gear teeth) across four (4) layer heights.

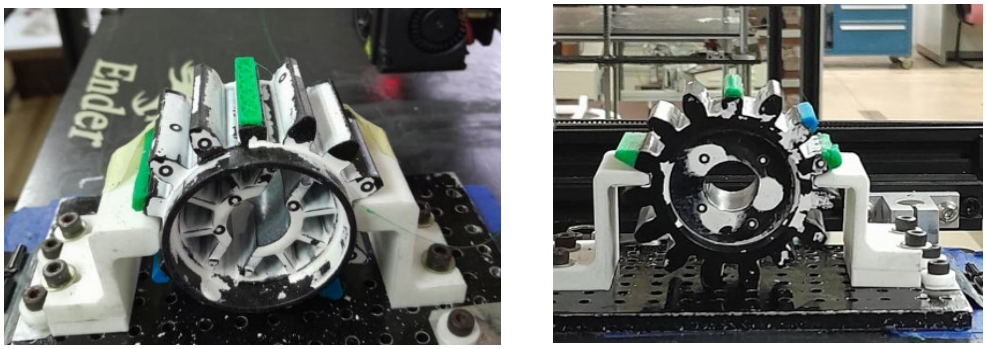

(a) (b)

Figure 5: (a) Gear placement on the fixture and (b) Reconstructed broken features.

Having fixed all the broken teeth, measurements of the parts' dimensional accuracy (DA) - height, width and length of the reconstructed and the original models' areas will be made.

4.2 Dimensional Accuracy (DA) and Surface Roughness (SR) Measurements

Dimensional accuracy is a key factor in 3D model reconstruction for 3D printing technology. The effects of filament type and layer height were found to affect the dimensional accuracy of the 3D-printed specimens [41]. They found that, based on dimensional measurements, the samples' length, height, and width were the most important factors to obtaining the most accurate results. The digital Vernier caliper was used to measure DA in the printed specimens, and the results showed that the most significant parameters include layer height, nozzle temperature, etc. [29]. In contrast, research was conducted on the development of the Dynamic Length Metrology (DLM) technique. During manufacturing, the micrometer was used to trace direct diameter measurements with accuracy [42]. In this study, focus was made on DA measurements and surface roughness (SA). Therefore, the parts' DA, including length, height, and width, were measured using a digital Vernier caliper and a micrometer at the varied layer heights (0.1 mm, 0.2 mm, 0.3 mm, and 0.4mm). Some selected DA measurements of length, height, and width using a Micrometer and a vernier caliper showed that the original tooth has a length of 34.75 mm, and the reconstructed parts have a length of 34.74 mm and a 0.1 mm layer height. While a 0.2 mm layer height of 15.011 mm, and a 0.3 mm layer height with a width of 5.506 mm.

4.3 Reconstructed Features (gear teeth) and their Labels

The reliability of the 3D printing machine in manufacturing was determined, in part, by dimensional accuracy measurements [43]. They conducted a theoretical-experimental analysis of the influence of FDM parameters on manufactured 3D parts made from PLA. After comparing their findings, such as showing positive average percentage deviations and the highest-accuracy thickness dimensions of some specimens, etc. They emphasized that focusing on parameter optimization has the potential to minimize standard deviation, thereby improving the dimensional accuracy of the manufactured 3D models. Based on these, the dimensional accuracy (DA) measurements were used to define and label the visual geometric features of the physically damaged part (PDP) positioned in the fixture, conforming to each reconstructed broken part. The evaluation focused on the primary geometric orientations, i.e., length, height, and width (Figure 6), as previously highlighted.

The demonstration of the original tooth with 15.010 mm height from the left, and four (4) digitally reconstructed broken feature parts onto the damaged surface areas of a real 3D part is shown in Figure 6. The first one has a layer height of 0.1 mm (17.716 mm), while the center one has a layer

height of 0.3 mm (14.531 mm). On the other hand, showing 15.011 mm of 0.2 mm layer height, and the last one with 14.539 mm is 0.4 mm layer height. Furthermore, the data (Figure 7) show the original part's geometric orientations and their values (length - 34.75 mm, height - 15.010 mm, width - 6.015 mm), and all the repaired models are displayed in various ways. The dimensional accuracy (DA) was good for the repaired model with a layer height of 0.1 mm, but it was higher than that of the other parts. The results indicate that the third one, which is 0.2 mm with a length of 34.76 mm, a height of 15.011 mm, and a width of 6.016 mm, is very close to the original feature part. On the other hand, parts with 0.3 mm layer heights showed a decrease, whereas 0.4 mm layer heights increased.

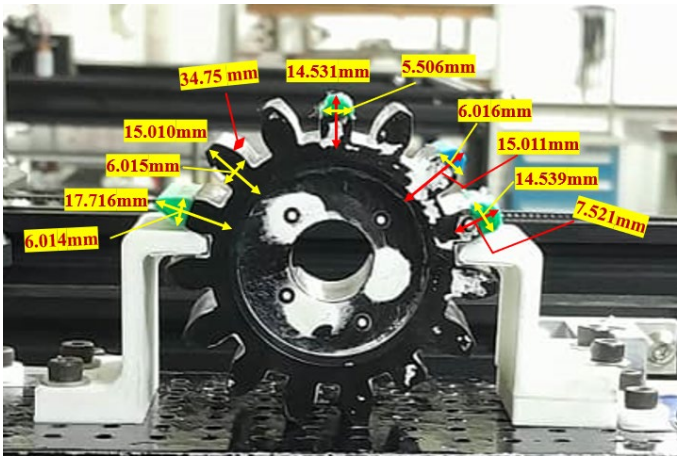

Figure 6: Displaying the dimensional measurement of reconstructed features.

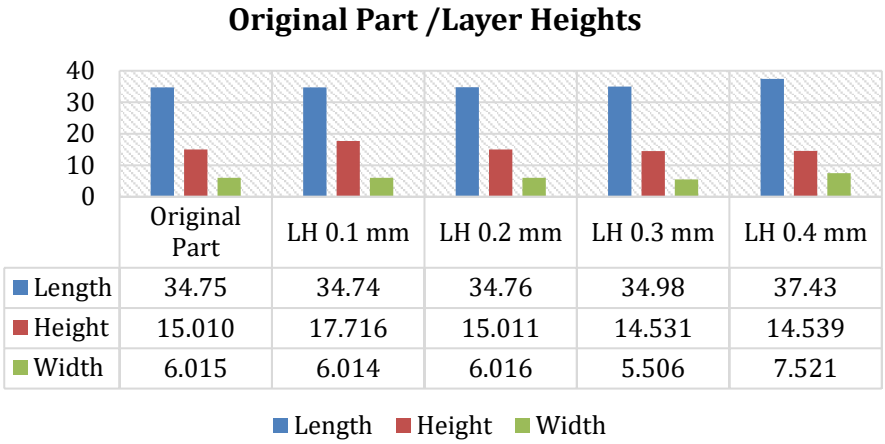

Figure 7: Chart representing dimensional accuracy data (DA) of the parts

4.4 Surface Roughness Measurements

Surface roughness plays a crucial role in determining the functionality and lifespan of a part [44]. The surface roughness measurements of the digital models were made with a Mitutoyo surface testing machine. However, the machine setup and other essential tasks were started prior to the measurements of the parts. When the measurements were conducted, the real physical model's surface roughness, represented by Ra and Rq, was 1.3355 µm and 1.6380 µm, respectively. At a 0.1 mm layer height, where Ra was 25.1742 µm and Rq was 30.6581 µm, the surface roughness was good and close to the real part. Additionally, the 0.2 mm layer height measurement showed lower surface roughness, with Ra of 21.2392 µm and Rq of 25.6308 µm. On the other hand, the layer height (0.3 mm) has Ra = 31.5703 µm, and Rq = 35.2642 µm, which indicates a harsh SR of the part. The last one is a 0.4 mm layer height, with Ra = 30.3206 µm and Rq = 34.9437 µm, which indicates the roughest surface of the part according to the results. Furthermore, Table 4 presents

a summary of the original model and layer heights employed by the measuring machine (Mitutoyo) to obtain the results.

Table 4: Pattern of surface roughness observed over different layer height.

S/n	Layer Height(s)	SR Findings
1	Original Part	a. Ra = 1.3355µm b. Rq = 1.6380µm
2	0.1 mm	a. Ra = 25.1742µm b. Rq = 30.6581µm
3	0.2 mm	a. Ra = 21.2392µm b. Rq = 25.6308µm
4	0.3 mm	a. Ra = 31.5703µm b. Rq = 35.2642µm
5	0.4 mm	a. Ra = 30.3206µm b. Rq = 34.9437µm

4.5 Comparison between Repair and Replacement

The comparison of costs between repaired damaged gear teeth and purchasing a new gear model is presented in Table 5. One feature repair costs RM 17.13, and purchasing a new part costs RM 40.00, which is 2.34 times cheaper and takes less than 2 hours to print. In this type of 3D printing repair, the technique consumes a small amount of PLA material, reduces material waste, and precisely repairs the broken part without having to replace the whole model[1].

Table 5: Comparison of Cost.

Option	Cost per Feature (MYR)	Savings Factor	Downtime Estimate
Repaired Feature	RM 17.13	2.34× cheaper	<2 hours
New Gear Purchase	RM 40.00	-	Days (sourcing)

The cost of repair is approximately 43% of the cost of replacement.

In summary, this method offers a strong basis for 3D-printed repairs on a variety of high-value components, but requires additional labor to make an accurate estimate. The gear case study's total costs amount to RM 17.13, primarily due to labor (88%), versus RM 40.00 for the replacement. This validates the process as practicable, cost-effective, adaptable for parts like pulleys, and sustainable for manufacturing.

5. CONCLUSIONS

In the repairs, a micrometer was employed to measure dimensional accuracy and surface roughness, and a sampling length evaluation was developed from the measuring machine (Mitutoyo). The results of the findings include:

i. The geometric orientations of the original molded, damaged part are 34.75 mm, 15.010 mm, and 6.015 mm, representing length, height, and width, respectively.
ii. DA for the repaired model with a layer height of 0.1 mm is good but appears higher than that of the other features.
iii. For the 0.2 mm part with 34.76 mm, 15.011 mm, and 6.016 mm (length, height, width), the results are the ones that are closest to the original feature.
iv. However, features with a 0.3 mm layer height showed a decrease, while those with a 0.4 mm layer height showed an increase.

On the issues of surface roughness measurements, the observations were made based on the following:

a) The original part's measurements showed that the surface roughness was Ra = 1.3355 μm and Rq = 1.6380 μm.
b) The SR for the repaired model with a layer height of 0.1 mm indicated that it was good, as it was near to the original part.
c) However, the 0.2 mm layer-height SR measurement showed lower surface roughness.
d) Then, a 0.3 mm layer height indicates a harsh SR for the part.

Based on the results, the 0.4 mm layer height's appearance specifies the roughest surface compared to other parts.

ACKNOWLEDGEMENT

I would like to acknowledge Professor Ahmad Baharuddin Abdullah for sponsoring the conference, and the Government of Nigeria, through Isa Kaita College of Education, Dutsin-ma, Katsina State, for shouldering the responsibilities of my PhD programme.

REFERENCES

[1] Chadha, C., Patterson, A. E., Allison, J. T., James, K. A., Jasiuk, I. M. Repair of high-value plastic components using fused deposition modeling. Proceedings of the 30th Annual International Solid Freeform Fabrication Symposium – An Additive Manufacturing Conference (2019) pp.1732–1755.
[2] Alhafeiti, H., Ziout, A., Alsaadiya, A., Alhebsi, A. Re-designing a gear using reverse engineering. Proceedings of the International Conference on Industrial Engineering and Operations Management, vol 2019 (2019) pp.1883–1892.
[3] Zong, Y., et al. A high-efficiency and high-precision automatic 3d scanning system for industrial parts based on a scanning path planning algorithm. Optics and Lasers in Engineering, vol 158 (2022) pp.107176.
[4] Song, L., Jiang, Q., Zhong, Z., Dai, F., Wang, G., Wang, X. Technical path of model reconstruction and shear wear analysis for natural joint based on 3d scanning technology. vol 188 (2022) pp.110584.
[5] Karganroudi, S. S., Aminzadeh, A., Ibrahim, H., Rahmatabadi, D., Francois, V., Cuillière, J. C. A novel automated approach for geometric reconstruction and flexible remanufacturing of spur gears using point cloud mapping analysis. Comput Aided Des Appl, vol 20, issue 1 (2023) pp.92–108.
[6] Parry, E. J., Best, J. M., Banks, C. E. Three-dimensional (3D) scanning and additive manufacturing (am) allows the fabrication of customized crutch grips. Mater Today Commun, vol 25 (2020) pp.2352-4928.
[7] Guo, X., Shi, Z., Yu, B., Zhao, B., Li, K., Sun, Y. 3d measurement of gears based on a line structured light sensor. Precis Eng, vol 61 (2020) pp.160–169.
[8] Rajaguru, K., Karthikeyan, T., Vijayan, V. Additive manufacturing-state of art. Mater Today Proc, vol 21 (2020) pp.628–633.
[9] Rabiu, A., Bawa, K. 3d printing technology as a means of self-reliance for technical education graduates in Kaduna, Nigeria. Northwest Journal of Educational Studies, vol 5, issue 1 (2022) pp.371304745.
[10] Mahamood, R. M., Jen, T. C., Akinlabi, S. A., Hassan, S., Akinlabi, E. T. Introduction to additive manufacturing technologies. Advances in Additive Manufacturing: Artificial Intelligence, Nature-Inspired, and Biomanufacturing (2023) pp.3-13.
[11] Shinde, A. A., Patil, R. D., Dandekar, A. R., Dhawale, N. M. 3d printing technology, material used for printing and its applications. International Journal of Scientific & Engineering Research, vol 11, issue 7 (2020) pp.105-108.

[12] Gojzewski, H., et al. Layer-by-layer printing of photopolymers in 3d: How weak is the interface? ACS Applied Materials & Interfaces, vol 12, issue 7 (2020) pp.8908-8914.
[13] Chadha, C., James, K., Jasiuk, I. M., Patterson, A. E. Extending the operating life of thermoplastic components via on-demand patching and repair using fused filament fabrication. Journal of Manufacturing and Materials Processing (JMPP), vol 6, issue 5 (2022) pp.103.
[14] Lakkala, P., Munnangi, S. R., Bandari, S., Repka, M. Additive manufacturing technologies with emphasis on stereolithography 3d printing in pharmaceutical and medical applications: A review. International Journal of Pharmaceutics: X, vol 5 (2023) pp.100159.
[15] Aprilia, A., Wu, N., Zhou, W. Repair and restoration of engineering components by laser directed energy deposition. Materials Today: Proceedings, vol 70 (2022) pp.206-211.
[16] Joo, H., Cho, S. Comparative studies on polyurethane composites filled with polyaniline and graphene for dlp-type 3d printing. Polymers (Basel), vol 12, issue 1 (2020) pp.67.
[17] Qian, J., et al. High-resolution real-time 360° 3d model reconstruction of a handheld object with fringe projection profilometry. Optics Letters, vol 44, issue 23 (2019) pp.5751-5754.
[18] NextEngine. Nextengine 3D scanner ultra HD. (2018).
[19] Qian, J., Feng, S., Tao, T., Hu, Y. High-resolution real-time 360◦ 3d surface defect inspection with fringe projection profilometry. Optics and Lasers in Engineering, vol 137 (2021) pp.106382.
[20] Hong, T. C., Ma'aram, A., Boon, O. J. High-accuracy cloud point scanning method based on a dual laser 3d scanner for head profile. Malaysian Journal of Fundamental and Applied Sciences, vol 18, issue 5 (2022) pp.558-569.
[21] Rašovic, N., Obad, M. A framework for optimal quality of parts in reverse engineering. Proceedings of the 27th DAAAM International Symposium, vol 27 (2016) pp.0328-0337.
[22] Autodesk Inc. To convert a mesh object to a 3d solid | Autocad 2016. (2026).
[23] Liu, Y., Zhao, Y., Liu, M., Sun, X. Parameterized high-precision finite element modelling method of 3d helical gears with contact zone refinement. Shock and Vibration, vol 2019, issue 1 (2019) pp.17.
[24] Palka, D. Use of reverse engineering and additive printing in the reconstruction of gears. Multidisciplinary Aspects of Production Engineering. MAPE 2020, vol 3, issue 1 (2020) pp.274–284.
[25] Nyuysoni, S. B., Mutua, J. M., Home, P. Mathematical model development and 3d printing of cylindrically shaped biofilm carrier media from recycled plastic waste for wastewater treatment. Journal of Environmental Protection, vol 13, issue 1 (2022) pp.15-31.
[26] Almudhaf, T. I. Design of automotive engine components by CAD software: Autodesk Inventor and SolidWorks. Journal of Engineering Research and Application, vol 10, issue 1 (2020) pp.25–31.
[27] Abdallah, R., et al. The use of SolidWorks in the evaluation of wind turbines in Palestine. Energy Nexus, vol 7 (2022) pp.100135.
[28] Kulczyk, T., et al. Computed tomography versus optical scanning: A comparison of different methods of 3d data acquisition for tooth replication. Biomed Research International, vol 2019, issue 1 (2019) pp.1-7.
[29] Muhammad, A. R., Sakura, R. R., Dwilaksana, D., Sumarji, Trifiananto, M. Layer height, temperature nozzle, infill geometry and printing speed effect on accuracy 3d printing PETG. R.E.M. (Rekayasa Energi Manufaktur) Jurnal, vol 7, issue 2 (2022) pp.81–88.
[30] Ultimaker. Ultimaker cura. (2023).
[31] Morettini, G., Palmieri, M., Capponi, L., Landi, L. Comprehensive characterization of mechanical and physical properties of PLA structures printed by FFF-3D-printing process in different directions. Progress Additive Manufacturing, vol 7, issue 5 (2022) pp.1111–1122.
[32] Kim, S. 3d model data generation and conversion for 3d printers. Journal of ELECTRONIC MATERIALS, vol 44, issue 3 (2015) pp.815–822.

[33] John, P., Komma, V. R., Bhore, S. P. Development of MATLAB code for tool path data extraction from the G-code of the fused filament fabrication (FFF) parts. Engineering Research Express, vol 5, issue 2 (2023) pp.025018.
[34] Maturkar, P. Design and development of 3d printer. International Journal of Scientific Research in Engineering and Management, vol 7, issue 4 (2023).
[35] Aljazara, A., et al. Quality of 3d printed objects using fused deposition modeling (FDM) technology in terms of dimensional accuracy. International Journal of Online and Biomedical Engineering (iJOE), vol 19, issue 14 (2023) pp.45-62.
[36] Biglete, E. R., et al. Dimensional accuracy evaluation of 3d - printed parts using a 3d scanning surface metrology technique. 2020 11th IEEE Control and System Graduate Research Colloquium ICSGRC (2020) pp.185–190.
[37] Tümer, E. H., Erbil, H. Y. Extrusion-based 3d printing applications of PLA composites: A review. Coatings, vol 11, issue 4 (2021) pp.390.
[38] Suhr, B., Skipper, W. A., Lewis, R., Six, K. Sanded wheel–rail contacts: Experiments on sand crushing behaviour. Lubricants, vol 11, issue 2 (2023) pp.38.
[39] Rezanezhad, S., Azadi, M. Impact of 3D-printed PLA coatings on the mechanical and adhesion properties of AM60 magnesium alloys. Composites Part C: Open Access, vol 12 (2023) pp.100415.
[40] Schneider, L., Gärtner, H. Additive manufacturing for lab applications in environmental sciences: Pushing the boundaries of rapid prototyping. Dendrochronologia (Verona), vol 76 (2022) pp.126015.
[41] Bolat, Ç., Ergene, B. An investigation on dimensional accuracy of 3d printed PLA, PET-G, and ABS samples with different layer heights. Çukurova Üniversitesi Mühendislik Fakültesi Dergisi, vol 37, issue 2 (2022) pp.449–458.
[42] Chiffre, L. D., et al. Accurate measurements in a production environment using dynamic length metrology (DLM). Procedia CIRP, vol 75 (2018) pp.343-348.
[43] Zisopol, D. G., Portoaca, A. I., Tanase, M. Dimensional accuracy of 3d printed dog-bone tensile samples: A case study. Engineering, Technology and Applied Science Research, vol 13, issue 4 (2023) pp.11400-11405.
[44] He, B., Ding, S., Shi, Z. A comparison between profile and areal surface roughness parameters. Metrology and Measurement Systems, vol 28, issue 3 (2021) pp.413–438.

Conflict of interest statement: The authors declare there is no conflict of interest.

Author Contributions Statement: Conceptualization, Methodology, Software, Formal Analysis, Investigation, Resources, Data Curation, Writing - Original Draft Preparation, Writing - Review & Editing - Muntaka M.; Supervision: Abdullah A.B.; Conference Sponsored: Abdullah A.B.